Measurement and Prediction of Helix-Loaded Chiral Composites

Colin R. Brewitt-Taylor, Peter G. Lederer, Frank C. Smith, and Sajad Haq

***Abstract*— A method is described for the extraction of the permittivity, permeability, and chirality of composite chiral materials, using measurements of reflection and transmission in a circular waveguide. This has been applied to a number of helix-loaded composites, in the frequency band 8–12 GHz. The properties of these composites have also been computed from the helix geometry and other basic information. The theory correctly predicts the frequency of the half-wavelength resonance observed, the relative magnitude of the constitutive parameters, and the low-frequency dielectric constant. But it has been found necessary to adjust the host-medium loss to obtain the correct absolute magnitudes. This agreement provides a confirmation that the theory is basically sound and so assists in discovering what chiral parameters are practically obtainable and in exploring applications of chiral materials.**

***Index Terms*—Chrial material, composite materials, helixes.**

I. Introduction

THERE has been an increasing interest in recent years in artificial chiral media for the microwave frequency range. Many possible applications have been proposed, for example radar absorbing materials [1], radomes [2], waveguides [3], and antennas [4]. An overview has been given by Cory [5]. In these initial theoretical explorations, apparently useful results have been obtained by the use of arbitrary chiral parameters. To put these explorations on a firmer foundation, it is necessary to discover what chiral parameters are obtainable in practice, and so establish whether the chirality can be made large enough for the applications envisaged. It is also necessary that no undesirable side effects are introduced along with the chirality.

In the present paper we report on the manufacture of a number of helix-loaded chiral samples, and the measurement of their constitutive parameters (complex permittivity, permeability, and chirality) using a circular waveguide. This provides practically realizable parameter values which can be used in theoretical explorations.

Now a chiral inclusion, such as a helix, produces contributions to all three constitutive parameters. Thus, the chirality cannot in practice be varied independently of the other parameters. Optimizations that allow arbitrary constitutive parameters are therefore likely to lead to unrealizable values. If possible, it is better to incorporate a theory of the constitutive parameters of the composite in terms of the basic properties of the host medium and the chiral inclusions. These basic parameters can be varied independently, and provided sensible values are chosen, it is then guaranteed that the composite constitutive parameters obtained are realizable.

We have previously [6], [7] used such a theory of chiral composites in an exploration of chiral radar absorbing materials. We here also report comparisons of the constitutive parameters predicted by this theory with the constitutive parameters measured by our circular waveguide method. This provides a test of the theory. In most respects the predictions do match the measured values, which shows that we do have a sound basic understanding of helix-loaded chiral composites. This provides a firm foundation for further exploration of possible applications.

II. Sample Fabrication

A number of chiral composites have been fabricated for measurement in circular guide in the frequency band 8–12 GHz [8]. These samples are in the form of disks, 23.3 mm in diameter, and approximately 3 mm thick. The samples were cast directly into the brass test-cells, to ensure a precise fit. The host material was Struers Epofix epoxy resin; this is transparent so as to allow visual inspection of the inclusions. Its dielectric constant was measured as $\epsilon = 2.90 - 0.07i$ in our circular waveguide. The helixes were made from stainless steel wire of 0.15 mm diameter. The "standard" helixes were 1.5 mm in height, and 1 mm in outside diameter, with three turns; though a number of variations on this have been used to explore the effects of changing parameters. Each disk contains from 50 to 250 helixes, which corresponds to metal fractions up to 2.5%. The helix dimensions were chosen to put the expected half-wavelength resonance within the frequency range of the measurement. The helix dimensions are similar to those used by Ro *et al.* [9], [10], but their measurements have been at much higher frequencies, so that their results are not directly comparable to ours.

The resin was degassed for a period of 40 min to reduce the number of bubbles. The helixes are added to the viscous resin individually and the resin is built up to the required total thickness in several layers. This procedure allows control of the orientation and concentration of the helixes and prevents settling and clumping. Some experimentation was required to determine optimum time and temperature for these procedures. The faces of the completed disk are polished to remove any

Manuscript received August 6, 1997; revised June 8, 1998.

C. R. Brewitt-Taylor and P. G. Lederer are with the Defense Evaluation and Research Agency, Malvern, U.K.

F. C. Smith is with the Department of Electronic Engineering, University of Hull, U.K.

S. Haq is with the Sowerby Research Centre, British Aerospace, Bristol, U.K.

Publisher Item Identifier S 0018-926X(99)04779-1.

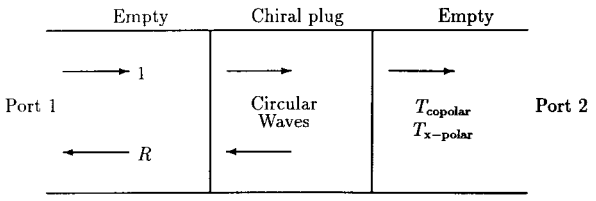

Fig. 1. Circular waveguide measurement.

meniscus and ensure the faces are parallel and flat. Since the resin is transparent, the completed sample can be visually inspected for bubbles and other defects.

Similar methods have been used for the fabrication of samples containing oriented helixes, which are then anisotropic, and for larger plate samples for free-space measurement. The waveguide method was chosen over free-space methods for these investigations because the sample required is much smaller, reducing the effort in fabrication.

III. Parameter Measurement in Circular Waveguide

A. Experimental Method

The experimental method is an extension of the standard method of measuring the complex permittivity and permeability of a conventional medium from the S-parameters of a sample filling a waveguide. Circular waveguide measurements have also been made in a similar manner by Jacob *et al.* [11], [12]. A medium having complex permittivity, permeability, and chirality will require a minimum of three complex S-parameter measurements to characterize the macroscopic properties of the material. In a chiral medium, the cross-polar transmission coefficient is nonzero. Thus, the necessary three measurements are obtained from the reflection coefficient R, the copolar transmission coefficient T_{co}, and the cross-polar reflection coefficient T_x. Theoretically, there should be no cross-polar reflection, since the medium is assumed isotropic and reciprocal.

A cylindrical plug of chiral material is placed into a section of circular waveguide propagating a single TE plane polarized mode (Fig. 1). The mode is launched in rectangular waveguide and fed to the circular waveguide through a rectangular-to-circular waveguide transition. The waveguide transition contains a section of resistive film to absorb any fields cross-polarized from the fields being measured: this prevents them being reflected from the waveguide transition back on to the sample, and so corrupting the S-parameter data.

The S-parameters are measured using an automatic network analyzer, which is calibrated using the usual TRL (through/reflect/line) calibration standards. Two sets of measurements are performed. One set has the two ports parallel, and gives values of the reflection and copolar transmission coefficients. In the second set the second waveguide port is rotated 45° relative to the first port, and modified TRL calibration is carried out. This gives a repeat measurement of the reflection coefficient and a 45° transmission coefficient T_{45}. The true 90° cross-polar transmission coefficient is then obtained from simple component resolving: $T_x = T_{45}\sqrt{2} - T_{co}$. The 90° transmission coefficient is not measured directly because the calibration cannot be carried out, since the through and line calibration measurements would give no signal with the ports at 90° to each other. In the results reported below, measurements were made from 8 to 12 GHz at intervals of 0.02 GHz. The measured S-parameters are smoothed to remove equipment-induced ripples, and every tenth value selected for further processing (giving an interval of 0.2 GHz). Some check on reproducibility is provided by the repeat measurements of the reflection coefficient and by the values of transmission coefficient in each direction through the sample, which should be the same by reciprocity.

B. Waveguide Modes

Consider a cylindrical plug of the chiral medium of length h entirely filling the radius a of a circular waveguide. We wish to extract the electromagnetic parameters from measurements of the reflection and two transmission coefficients. We first tackle the forward problem of calculating the transmission and reflection from a known medium. We find the propagating modes in the waveguide, and then use the usual field boundary conditions to find the reflection and transmission coefficients [13].

In our work we shall use the following set of constitutive relations:

$$\begin{aligned}\mathbf{D} &= \epsilon\mathbf{E} - i\chi\mathbf{H} \\ \mathbf{B} &= i\chi\mathbf{E} + \mu\mathbf{H}.\end{aligned} \tag{1}$$

Here the parameter χ is the chirality, with the symbol chosen for its mnemonic value. The factor i is introduced so that the chirality is real in a lossless medium. It is assumed that the helixes are randomly oriented, so that the medium is isotropic. This form of constitutive relations is similar to those used by Sihvola and Lindell [14], [15]. When we come to display values of the constitutive parameters, we will normalize the permittivity to ϵ_0 and the permeability to μ_0 in the usual way, and normalize the chirality to $\sqrt{\mu_0\epsilon_0}$. The relative values are then of order unity, and it is easier to judge the magnitude of the values obtained.

The procedure for finding the waveguide modes is parallel to that of Hollinger *et al.* [16], amended as necessary for our different constitutive relations. Starting from Maxwell's curl-equations, we make the change of variables known as Bohren's decomposition $\mathbf{U} = \mathbf{E} + iZ\mathbf{H}$ and $\mathbf{V} = \mathbf{E} - iZ\mathbf{H}$. The new variables $\mathbf{U}$ and $\mathbf{V}$ are related to left- and right-circular polarized waves. Introducing the usual pseudo-wavenumber $k = \omega\sqrt{(\epsilon\mu)}$ and impedance $Z = \sqrt{(\mu/\epsilon)}$, we obtain separate equations for $\mathbf{U}$ and $\mathbf{V}$ as follows:

$$\begin{aligned}\text{curl } \mathbf{U} &= k_u\mathbf{U} \qquad \text{with } k_u = -k + \omega\chi \\ \text{curl } \mathbf{V} &= k_v\mathbf{V} \qquad \text{with } k_v = +k + \omega\chi.\end{aligned} \tag{2}$$

The constants k_u and k_v are recognized as the wavenumbers of circularly polarized plane-waves in an infinite chiral medium.

We now look for solutions of these curl-equations in the form: $U(r, \theta, z) = U(r)e^{im\theta - ipz}$. Here m is an integer constant giving the azimuthal order of the solution (we shall need only $m = \pm 1$); and p is the wavenumber of propagation

along the z-direction (the length of the waveguide). Writing these equations in cylindrical coordinates, we find that U_z obeys Bessel's differential equation, and so has solutions $U_z = A_u J_m(q_u r)$, with $q_u^2 = k_u^2 - p^2$ and A_u a constant. The other components of $\mathbf{U}$ are obtained from the curl-equations. The analysis for the V equation is exactly parallel. We then construct expressions for E_z and E_θ from the U and V solutions, with two constants A_u and A_v

$$\begin{aligned}
E_z &= \frac{A_u}{2} J_m(q_u r) + \frac{A_v}{2} J_m(q_v r) \\
E_\theta &= \frac{mp}{2r}\left(\frac{A_u}{q_u^2} J_m(q_u r) + \frac{A_v}{q_v^2} J_m(q_v r)\right) \\
&\quad - \frac{1}{2}\left(\frac{A_u k_u}{q_u} J'_m(q_u r) + \frac{A_v k_v}{q_v} J'_m(q_v r)\right) \\
E_r &= \frac{im}{2r}\left(\frac{A_u k_u}{q_u^2} J_m(q_u r) + \frac{A_v k_v}{q_v^2} J_m(q_v r)\right) \\
&\quad - \frac{ip}{2}\left(\frac{A_u}{q_u} J'_m(q_u r) + \frac{A_v}{q_v} J'_m(q_v r)\right). \qquad (3) \\
H_z &= \frac{-i}{2Z}(A_u J_m(q_u r) - A_v J_m(q_v r)) \\
H_\theta &= \frac{-imp}{2rZ}\left(\frac{A_u}{q_u^2} J_m(q_u r) - \frac{A_v}{q_v^2} J_m(q_v r)\right) \\
&\quad + \frac{i}{2Z}\left(\frac{A_u k_u}{q_u} J'_m(q_u r) - \frac{A_v k_v}{q_v} J'_m(q_v r)\right) \\
H_r &= \frac{m}{2rZ}\left(\frac{A_u k_u}{q_u^2} J_m(q_u r) - \frac{A_v k_v}{q_v^2} J_m(q_v r)\right) \\
&\quad - \frac{p}{2Z}\left(\frac{A_u}{q_u} J'_m(q_u r) - \frac{A_v}{q_v} J'_m(q_v r)\right). \qquad (4)
\end{aligned}$$

Here $J'_m(\xi)$ means the derivative with respect to the total argument $dJ_m(\xi)/d\xi$, rather than with respect to the radius $dJ_m(\xi)/dr$.

These solutions depend on the propagation constant p which is so far unknown. The boundary conditions are that the tangential components of electric field are zero on the metal waveguide wall. Each condition fixes the ratio A_u/A_v, and requiring that these be consistent leads to

$$\begin{aligned}
&mp(q_u^2 - q_v^2) J_m(aq_u) J_m(aq_v) + ak_u q_u q_v^2 J_m(aq_v) J'_m(aq_u) \\
&\quad - ak_v q_u^2 q_v J_m(aq_u) J'_m(aq_v) = 0. \qquad (5)
\end{aligned}$$

We then find the propagation constant p by iteratively solving this equation. Since the Bessel functions are oscillatory, there is a series of possible solutions, one for each mode. For chiral media, it is not obvious what starting value to use for the iteration. Our software always starts with a nonchiral medium, for which this equation simplifies, and is solved when either $J_m(qa) = 0$ or $J'_m(qa) = 0$. Since the zeros of Bessel's function and its derivative are known, we can guarantee the correct solutions in the nonchiral case. The software then increases the chirality in small steps up to the desired value, using the solution for the previous chirality to start the next solution and thus ensuring that the different solutions are followed. The program also checks that the solutions obtained are different: otherwise the method would fail later on. Once the propagation constant p_n for each mode has been found, one obtains q_u and q_v, and hence the ratio A_u/A_v from the boundary condition equations. We also need the modes for air-filled part of the waveguide, which can be obtained as the nonchiral special case of the above theory.

C. Boundary Matching

At the boundaries on each end of the plug, the waves must satisfy the usual tangential field continuity conditions. Modes with different azimuthal number m are orthogonal, and so are not mixed at the boundary. But modes with different mode number n are mixed because mode n does not have the same radial variation in nonchiral and chiral media. This is a new complication arising with the chirality. Thus, we cannot solve the boundary problem for each radial mode separately, but must solve for all modes simultaneously. We do this by least squares matching at several radial positions, with the number of points at least equal to the number of radial modes taken into account. For each mode, there are four unknown wave amplitudes (reflected, transmitted, and up and down in the plug), assuming unit incident wave. But there are eight boundary conditions, namely those on E_θ, E_r, H_θ, and H_r, and the two faces $z = 0$ and $z = h$ of the plug. These boundary conditions are presumably not all independent, but it is not obvious what subset of them is sufficient. We have simply included them all in the least squares fitting. Our method differs from that of Jacob [11] in that we perform mode matching at the two faces of the plug simultaneously, whereas he treats each boundary separately. This includes coupling of the two faces by higher order modes, which may be propagating rather than evanescent in a high-dielectric sample.

We have found that four modes and eight matching radii are sufficient for the present purpose, in that using more modes or matching radii does not significantly affect the reflection and transmission coefficients obtained. This is similar to the requirement of five modes mentioned by Busse and Jacob [17]. Inspection of the matched fields at the plug boundaries shows evidence of difficulty at the waveguide wall. We suspect that there is a field singularity at this junction of three media: the chiral plug, the air, and the waveguide metal. However, this does not appear to upset the reflection and transmission calculation.

The above analysis is carried through for $m = 1$ and for $m = -1$, corresponding to left and right circularly polarized incident waves. The ratios of coefficients for $n = 1$ in the air-filled guide give the reflection and transmission coefficients of the dominant mode. These must then be combined in the usual way to give the S-parameters for the plane polarized waves used in the measurements.

The inverse problem of finding the properties of the chiral plug is then solved by iterative fitting of the properties to the measured S-parameters. The standard parameter extraction procedure for nonchiral media is used to obtain starting values of permittivity and permeability, and the starting chirality is always zero, as explained above. Since the samples are thin, we are not seriously troubled by the ambiguity in this method: there is usually only one plausible solution. Alternatively, if the measurement has been made at a series of frequencies, the extracted parameters for the previous frequency can be used

for starting values, together with the previous mode propagation constants. The number of iterations required varied from 5 to 30, with high chirality samples requiring more iterations. A series of 19 frequency points, as used below, takes 30–60 min on a Sun workstation, but little manual intervention is required.

IV. Predictions from Helix Geometry

We will now describe the method of predicting the composite's constitutive parameters from the geometry of the helixes and other basic information. The method has been previously described [6], [7], and so will only be outlined here. Similar methods have also been used by several other authors [18]–[21]. The method-of-moments program NEC [22] is used to carry out an analysis of a single inclusion. We then calculate the effective medium parameters of a composite material containing such inclusions, and compare this to the values measured by the method described above.

The computer program NEC can compute the current distribution in a given wire structure, in response to any incident plane wave. Once the current has been computed, a separate computer program is used to compute the electric moment $\mathbf{p_e}$ and magnetic moment $\mathbf{p_m}$ by numerical integration. The moments are

$$\mathbf{p_e} = \frac{1}{i\omega} \int \mathbf{I}\, dl$$
$$\mathbf{p_m} = \tfrac{1}{2} \int I\mathbf{r} \times d\mathbf{r}. \tag{6}$$

Here $\mathbf{r}$ is the vector from an origin to an element of the current, and $d\mathbf{r}$ is the vector element of length pointing along the wire; $\mathbf{I}$ is the current in the wire and I its magnitude; and ω is the angular frequency. Guérin [20] and Luebbers [21] use an alternative method of obtaining the polarizabilities, via the forward and backward scattered fields. The two methods are equivalent, neglecting mutual coupling between the helixes. Our method can easily be extended to compute the quadrupole and higher moments, which recent work suggests is necessary for anisotropic chiral composites [23].

There are in general four complex polarizability tensors, relating the induced electric and magnetic moments to the incident electric and magnetic fields

$$\mathbf{p_e} = \alpha_{ee}\epsilon_0\mathbf{E} + \alpha_{em}\epsilon_0 Z_0\mathbf{H}$$
$$\mathbf{p_m} = \alpha_{me}\mathbf{E}/Z_0 + \alpha_{mm}\mathbf{H}. \tag{7}$$

Here α_{ee} is the usual electric polarizability, and α_{mm} is the usual magnetic polarizability; these both have dimensions of volume. There are two cross-polarizabilities α_{em} and α_{me}, which we have defined with factors of ϵ_0 and Z_0 (the impedance of free-space) introduced to give all the polarizabilities the same dimensions of volume.

These four 3×3 tensors have 36 components between them. We can apply six different incident plane waves to the object (up and down each of the three axes), with two polarizations each. For each incident wave we can compute the three components each of $\mathbf{p_e}$ and $\mathbf{p_m}$. Thus, there are 72 complex values available, which is more than enough to find the 36 polarizability components. We use pairs of oppositely directed waves (Fig. 2) to find the effects of the separate fields by adding and subtracting the dipole moments obtained with each of the pairs. For example, in Fig. 2, adding the results of waves 1 and 2 will yield the effects of E_x, namely the three electric polarizabilities $(\alpha_{ee})_{ix}$ and the three cross-polarizabilities $(\alpha_{me})_{ix}$ (for $i = x, y, z$), with the effect of H_y cancelling out. Subtracting this pair cancels the E_x effect and yields the H_y effects, namely the magnetic polarizabilities $(\alpha_{mm})_{iy}$ and the cross-polarizabilities $(\alpha_{em})_{iy}$. Similar adding and subtracting for the other wave-pairs yields all the 36 polarizabilities. There are two wave-pairs which yield any particular polarizability: both values are computed, and the average taken. The polarizabilities are frequency dependent, so the above procedure is carried out at each frequency of interest.

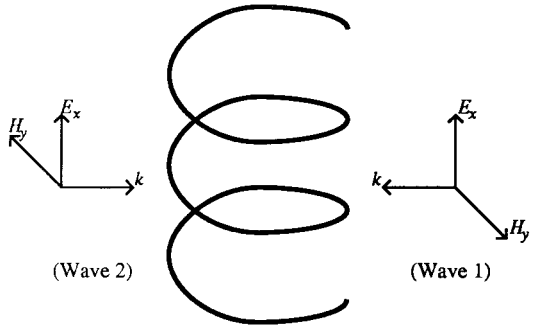

Fig. 2. Incident waves for extraction of polarizabilities.

Having obtained the tensor polarizabilities, we average the diagonal components to obtain the (scalar) polarizabilities of a randomly oriented collection of particles, and discard the off-diagonal components, which will average to zero.

The version of the NEC program used allows the complex dielectric constant of the host medium to be specified. Thus we can incorporate loss in the host medium, rather than in the helix wire as was done in the previous work [7]. The scaling procedure previously used to account for a real host dielectric constant is no longer necessary.

We now proceed from the particle polarizabilities α_{ee}, α_{mm}, α_{em}, and α_{me}, to the effective permittivity, permeability, and chirality of the composite medium. The treatment is adapted from that given in [15] for spherical chiral particles, which is a generalization of the usual Clausius–Mossotti derivation for the dielectric constant of composite media. The local fields at any helix are assumed to differ from the applied fields by one-third of the polarization, as in the standard Clausius–Mossotti theory. With this assumption we arrive at the following formulas for the properties of the composite medium

$$\epsilon = \epsilon_0 \frac{(1 + 2n\alpha_{ee}/3)(1 - n\alpha_{mm}/3) + 2n^2\alpha_{em}\alpha_{me}/9}{(1 - n\alpha_{ee}/3)(1 - n\alpha_{mm}/3) - n^2\alpha_{em}\alpha_{me}/9}$$
$$\mu = \mu_0 \frac{(1 + 2n\alpha_{mm}/3)(1 - n\alpha_{ee}/3) + 2n^2\alpha_{em}\alpha_{me}/9}{(1 - n\alpha_{ee}/3)(1 - n\alpha_{mm}/3) - n^2\alpha_{em}\alpha_{me}/9}$$
$$\chi = \chi_0 \frac{in\alpha_{em}\sqrt{\epsilon_0\mu_0}}{(1 - n\alpha_{ee}/3)(1 - n\alpha_{mm}/3) - n^2\alpha_{em}\alpha_{me}/9}. \tag{8}$$

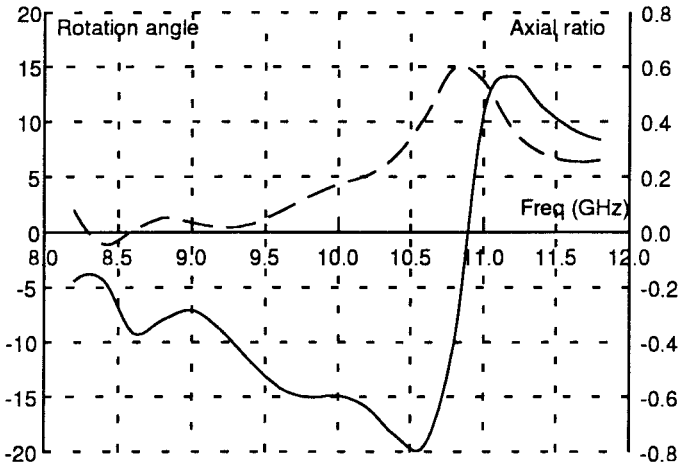

Fig. 3. Measurement of sample containing 50 right-hand helixes.

The same formulas have also been given by Sauviac *et al.* [19] and by Guérin [20]. This Clausius–Mossotti treatment is an approximation, and its success is an open question. There exist several more sophisticated approximate homogenization methods, or the much more computationally intensive but physically complete method of Whites [24]. These properties are frequency-dependent, through the underlying helix polarizabilities.

V. Comparisons of Measured and Predicted Parameters

Samples have been fabricated with varying concentrations of helixes, both left and right handed and a mixture and also with different pitches. The first set of helixes had an outside cylinder diameter of 1 mm and a cylinder length of 1.5 mm, with three right-hand turns. Other dimensions are given in Section II. The first sample to be discussed had 50 right-handed helixes in a disk 2.83 mm thick, which corresponds to 0.60% of metal in the sample, so that it is a fairly low concentration. We can easily compute the rotation of the plane of polarization θ, and the axial ratio of the elliptically polarized transmitted wave $\tan\psi$, by the formulas [25]

$$\tan 2\theta = \frac{2a_x a_y \cos\delta}{a_x^2 - a_y^2}$$

$$\sin 2\psi = \frac{2a_x a_y \sin\delta}{a_x^2 + a_y^2} \tag{9}$$

where $a_x = |T_{co}|$, $a_y = |T_x|$, and $\delta = \arg T_x - \arg T_{co}$.

Fig. 3 shows the angle of rotation and the axial ratio for this sample. The angle of rotation is small at low frequencies, and goes negative to about $-15°$ at 10.8 GHz. It then passes through zero, to $+15°$ at 11.5 GHz. This sign reversal is related to the resonant behavior of the current in the helix wire, which is a half-wavelength long at 10.8 GHz. Similar variations have been observed by other workers, e.g., [26], going back to the early work of Lindman [27], [28] and of Tinoco *et al.* [20]. The axial ratio stays near zero (linearly polarized) at low frequency and rises to about 0.25 at a frequency near the zero-crossing of the rotation angle. At this frequency the chirality is pure imaginary, so that there is differential absorption between the left- and right-hand circular waves, leading to the observed departure from linear polarization.

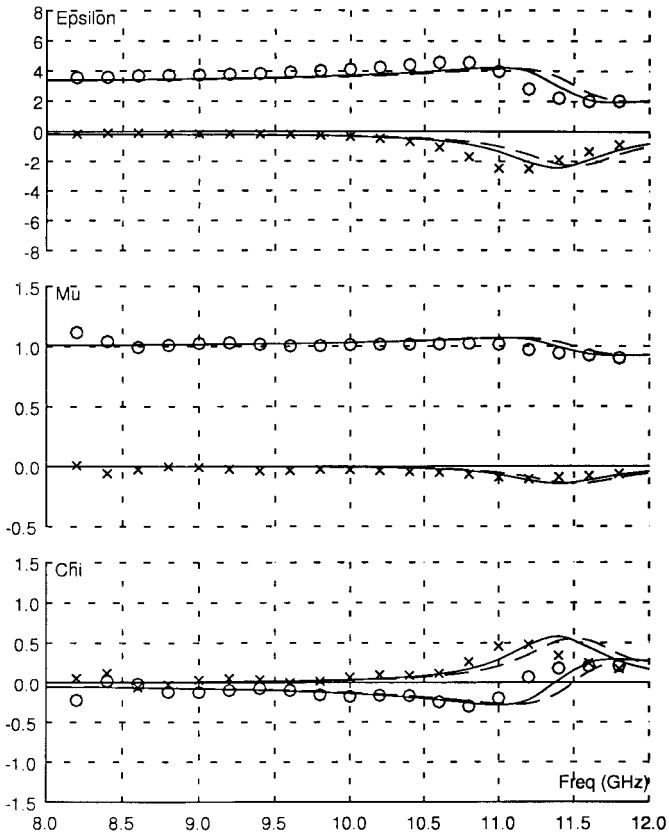

Fig. 4. Constitutive parameters for 50 right-handed helixes. Measured values: real part (circles) and imaginary part (crosses). Computed: with interactions (solid), without interactions (broken).

Fig. 4 shows the relative permittivity, permeability, and chirality obtained from the process described in Section III, for this same sample. Each of the permittivity, permeability, and chirality show a resonant behavior, though the effect on permeability is small. The real parts rise slowly to 10.8 GHz, then fall to 11.8 GHz, with chirality passing through zero and permittivity passing lower than the host medium at 11.3 GHz. The imaginary parts show maximum negative excursion in the same frequency range.

The solid lines on the graphs show the predictions made by the method of Section IV. It was found that a prediction using the observed host dielectric constant of $\epsilon_r = 2.9 - 0.07i$ gave resonances that were at the right frequency, but too large in magnitude. The predictions shown were obtained by increasing the imaginary (loss) part from $-0.07i$ to $-0.15i$. A fairly good fit is then obtained. Apart from this adjustment of the loss, the prediction proceeds from measurable geometric and other basic quantities, with no other adjustable parameters. It is then pleasing to see that the prediction gives the correct low-frequency dielectric constant, the correct resonant frequency, and the correct relative magnitudes of the three constitutive parameters, including their real and imaginary parts. This provides confidence that the prediction method is basically sound. Future work could include an error analysis of the

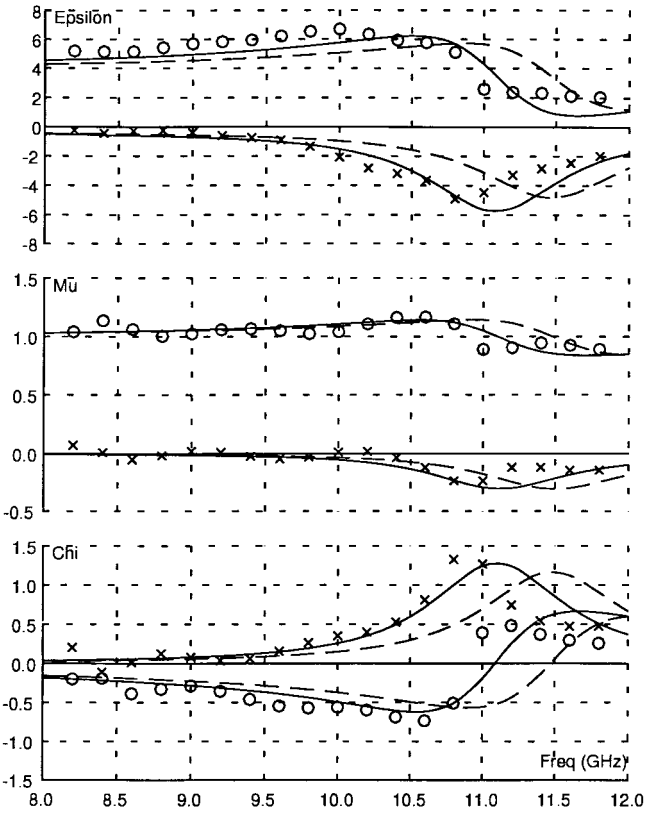

Fig. 5. Constitutive parameters for 150 right-handed helixes. Measured values: real part (circles) and imaginary part (crosses). Computed: with interactions (solid), without interactions (broken).

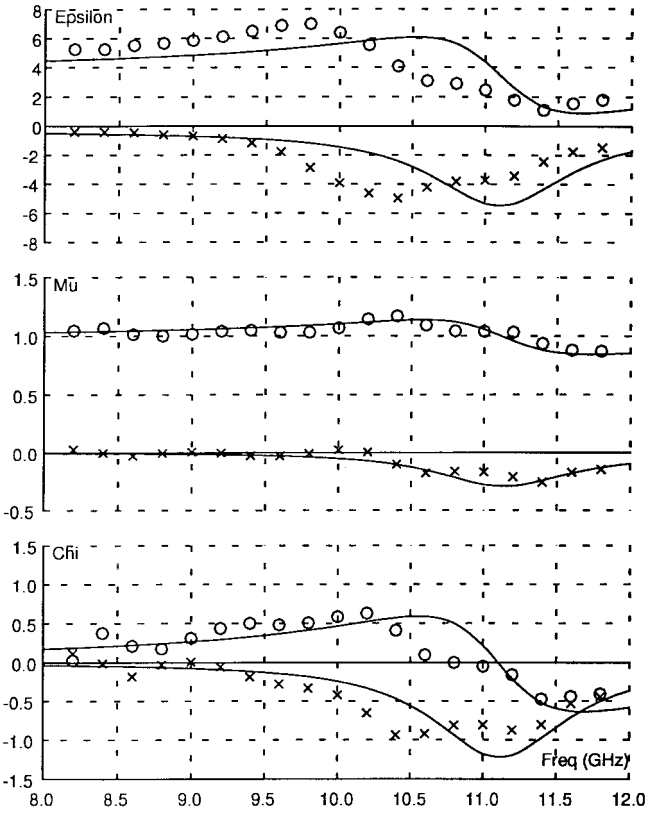

Fig. 6. Constitutive parameters for 150 left-handed helixes. Measured values: real part (circles) and imaginary part (crosses). Computed: with interactions (solid line).

measurements, on the lines of Smith *et al.* [30], so that error bars could be provided on the comparison graphs.

Moving to higher concentration, Fig. 5 shows the constitutive parameters for a sample containing 150 helixes in a 2.71-mm-thick disk, giving a metal fraction of 1.87%. The chirality is nearly three times as large in this sample, with maximum relative magnitude of 1.4 at 10.8 GHz. This is roughly proportional to the helix concentration, as might be expected. For this sample a prediction using Im $\epsilon_r = -0.07$ gives much too large a resonance, and to get the fit shown it was necessary to increase the host medium loss to Im $\epsilon_r = -0.25$. This adjustment is much more than required for the previous low concentration sample. Thus, this error becomes more important as the concentration is increased, which suggests that it is due to an inaccurate treatment of mutual interactions between the helixes. In the figure, the solid lines show the prediction including the interaction treatment after Clausius–Mossotti, described above. The broken lines show the prediction without this correction, i.e., equating the local field at each helix with the applied field. The correction has little effect at low concentration (Fig. 4), but has a significant effect at this higher concentration. In particular the Clausius–Mossotti correction gives a better resonant frequency fit, and so does improve the prediction.

Next we change the handedness of the helixes: Fig. 6 shows the constitutive parameters for a sample containing 150 left-hand helixes in a disk of 2.82 mm thickness, giving a metal concentration of 1.80%. The prediction is the same as for the previous sample (Fig. 5), except that the sign of chirality is reversed. This reversal of sign is indeed seen in the measured parameters. The magnitude of the measured parameters is similar to the right-handed helixes, but the measured resonant frequency is somewhat lower, for reasons that are not understood at present.

Fig. 7 shows the constitutive parameters for a mixture of 75 left-handed and 75 right-handed helixes in a disk of 2.77 mm thickness, giving a metal fraction of 1.83%. The prediction has the same permittivity and permeability as before, but with zero chirality. The measured results show similar magnitudes of permittivity and permeability and randomly varying chirality.

We have also fabricated some samples with varying helix pitch. As an example, Fig. 8 shows the constitutive parameters for a sample containing 100 right-hand helixes with a cylinder length of 0.75 mm, i.e., half the pitch of the previous samples. The disk is 3.04 mm thick, giving a metal fraction of 1.11%. This effect on permittivity and chirality is comparatively small for this sample. The helix shape is much more compressed than that for maximum chirality: the ratio of pitch to wire length is only about 0.1 instead of the optimum value of 0.55 [7], [31]. The predicted results agree with this and they also correctly give the downwards shift of resonant frequency, which is presumably due to mutual coupling between the turns of the helixes.

Finally, Fig. 9 shows the results for a sample containing 100 long-pitch helixes, which have a cylinder length of 3 mm,

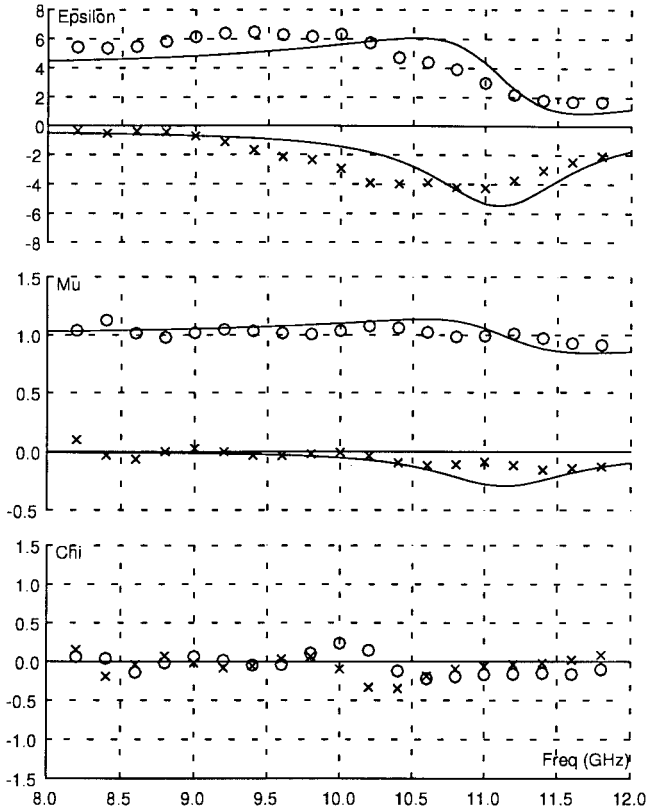

Fig. 7. Constitutive parameters for 150 mixed helixes. Measured values: real part (circles) and imaginary part (crosses). Computed: with interactions (solid line).

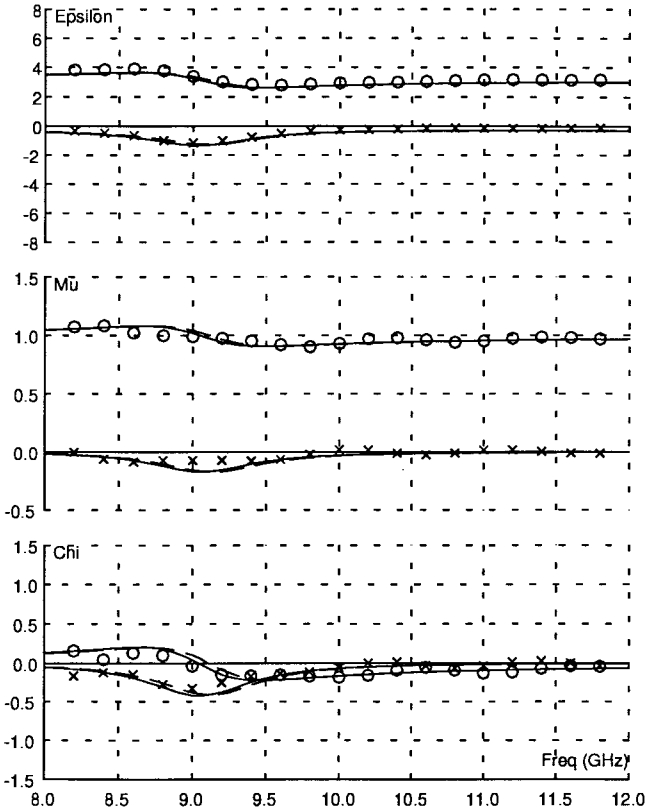

Fig. 8. Constitutive parameters for 100 0.25-mm-pitch helixes. Measured values: real part (circles) and imaginary part (crosses). Computed: with interactions (solid), without interactions (broken).

and so twice the pitch of the first samples. We see that the permittivity and chirality effects are indeed larger than the short-pitch samples of Fig. 8. It is also noticeable that in this case the prediction without Clausius–Mossotti correction gives a better fit than that with the correction. The Clausius–Mossotti correction field correction of 1/3 of the polarization assumes a spherical hole around the particle, whereas the present helixes have an aspect ratio of 3 : 1. The correction may be inaccurate for such elongated particles.

VI. Conclusions

In this paper we have reported results from the measurement of a number of helix-loaded chiral samples using a circular waveguide apparatus. This is a generalization of the standard waveguide method for nonchiral materials. The reflection coefficient, and copolar and cross-polar transmission coefficients are measured, and from these we can extract the complex permittivity, permeability, and chirality of the samples. The computation required for the parameter extraction is considerable, but quite practicable for modern computers. The constitutive parameters show resonant behavior when the wire length is half a wavelength in the host medium. Chirality values up to $1.5\sqrt{\epsilon_0 \mu_0}$ have been observed, in samples whose dielectric constant varies from the host medium value of 2.9 to a maximum of about 7.

We have also reported comparisons of these measurements with predictions starting from the geometry of the helixes and other basic information. The predictions give the correct low-

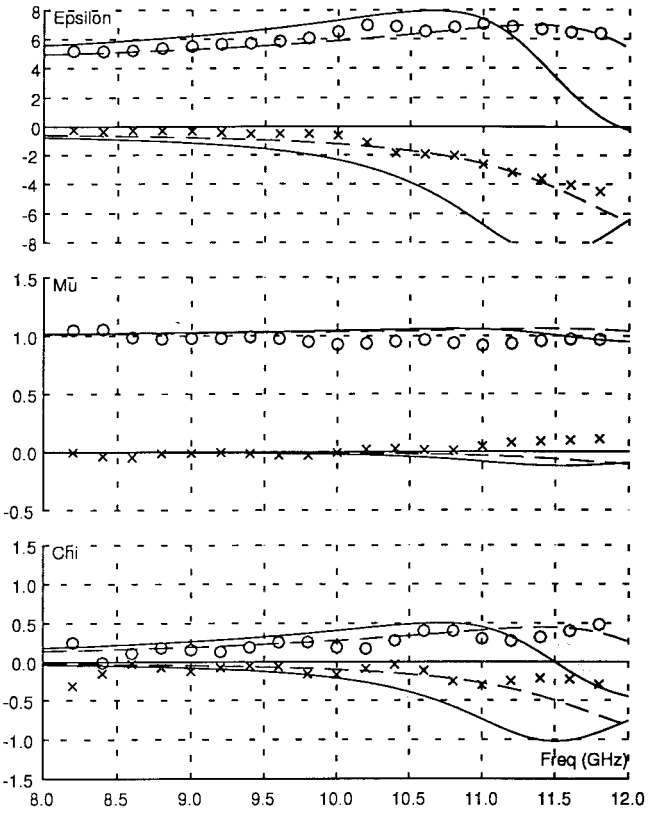

Fig. 9. Constitutive parameters for 100 1.0-mm-pitch helixes. Measured values: real part (circles) and imaginary part (crosses). Computed: with interactions (solid), without interactions (broken).

frequency dielectric constant, the correct resonant frequency, and the correct relative magnitude of the permittivity, permeability, and chirality, and of their real and imaginary parts. But it was found necessary to increase the imaginary part of the host medium dielectric constant to give the correct absolute magnitudes of the constitutive parameters. The cause of this discrepancy is not understood, but the fact that it gets worse with increasing helix concentration suggests that it is an effect of mutual coupling between the helixes. Further attention to this point in needed in future work, exploring the available more sophisticated homogenization techniques. We have discussed samples with varying helix concentration; left-handed and right-handed and mixed helixes; and varying pitch. Apart from the adjustment of host medium loss, the prediction proceeds from known basic information, and its success in the various cases considered confirms that it is generally sound.

Together, the prediction and measurement method provide a firm foundation for exploration of possible applications of chiral media.

REFERENCES

[1] V. K. Varadan, V. V. Varadan, and A. Lakhtakia, "On the possibility of designing anti-reflection coatings using chiral composites," *J. Wave-Material Interaction*, vol. 2, no. 1, pp. 71–81, 1987.

[2] H. Cory and I. Rosenhouse, "Minimization of reflection coefficient at feed of radome-covered reflector antenna by chiral device," *Electron. Lett.*, vol. 27, no. 25, pp. 2345–2347, 1991.

[3] P. Pelet and N. Engheta, "The theory of chirowaveguides," *IEEE Trans. Antennas Propagat.* , vol. 38, pp. 90–98, 1990.

[4] D. L. Jaggard, J. C. Liu, A. Grot, and P. Pelet, "Thin wire antennas in chiral media," *Electron. Lett.*, vol. 27, pp. 243–244, 1991.

[5] H. Cory, "Chiral devices—An overview of canonical problems," *J. Electromag. Waves Appl.*, vol. 9, pp. 805–829, 1995.

[6] C. R. Brewitt-Taylor, "Modeling of helix-loaded chiral radar absorbing layers," in *Proc. PIERS-93 Conf.*, Pasadena, CA, July 12–16, 1993, p. 529.

[7] ———, "Modeling of helix-loaded chiral radar-absorbing layers," in *PIERS Book Series Vol. 9, Bianisotropic and Bi-Isotropic Media and Applications*, A. Priou, Ed., 1994.

[8] S. Haq and D. L. Tunnicliffe, "Fabrication of chiral composites for waveguide and free-space measurements," in *Proc. Chiral-95 Conf.*, Pennsylvania State University, Oct. 11–14, 1995, pp. 21–26.

[9] R. Ro, V. V. Varadan, and V. K. Varadan, "Electromagnetic activity and absorption in microwave chiral composites," in *Proc. Inst. Elect. Eng.*, 1992, vol. 139, pt. H, no. 5, pp. 441–448.

[10] V. V. Varadan, R. Ro, and V. K. Varadan, "Measurement of the electromagnetic properties of chiral composite materials in the 8–40 GHz range," *Radio Sci.*, vol. 29, no. 1, pp. 9–22, 1994.

[11] J. Reinert, G. Busse, and A. F. Jacob, "A procedure to extract the chirality parameter from waveguide measurements," in *Proc. Chiral-95 Conf.*, Pennsylvania State University, June 1995, pp. 9–12.

[12] G. Busse, J. Reinert, M. Klemt, and A. F. Jacob, "On chirality measurements in circular waveguides," in *Advances in Complex Electromagnetic Materials*, A. Priou Ed., 1997, pp. 333–339.

[13] C. R. Brewitt-Taylor, P. G. Lederer, and F. C. Smith, "Measurement of chiral media in a circular waveguide," in *Proc. Chiral-94 Conf.*, Périgueux, France, May 18–20, 1994, pp. 413–416.

[14] A. H. Sihvola and I. V. Lindell, "Bi-isotropic constitutive relations," *Microw. Opt. Technol. Lett.*, vol. 4, no. 8, pp. 295–297, 1991.

[15] ———, "Chiral Maxwell–Garnet mixing formula," *Electron. Lett.*, vol. 26, no. 2, pp. 118–119, 1990.

[16] R. Hollinger, V. V. Varadan, and V. K. Varadan, "Eigenmodes in a circular waveguide containing an isotropic chiral material," *Radio Sci.*, vol. 26, no. 5, pp. 1335–1344, 1991.

[17] G. Busse and A. F. Jacob, "Lossy chiral slabs in circular waveguide," in *Proc. Inst. Elect. Eng. Micro. Antennas and Propag.*, 1996, vol. 143, no. 1, pp. 51–56.

[18] L. R. Arnaut and L. E. Davis, "On planar chiral structures," in *Proc. PIERS-95 Conf.*, Seattle, WA, July 24–28, 1995, p. 165.

[19] B. Sauviac, F. Mariotte, J-P. Héliot, A. Riboulet, "Numerical modeling of heterogeneous materials with dielectric or magnetic chiral inclusions," in *Proc. Chiral'95 Conf.*, Pennsylvania State University, Oct. 11–14, 1995, pp. 35–41.

[20] F. Guérin, P. Bannelier, and M. Labeyrie, "Scattering of electromagnetic waves by helixes and application to the modeling of chiral composites—Part I: Simple effective medium theories, and—Part II: Maxwell–Garnet treatment," *J. Phys. D: Appl. Phys.*, vol. 28, pp. 623–642 and pp. 643–656, 1995.

[21] R. Luebbers, H. S. Langdon, F. Hunsberger, and C. F. Bohren, "Calculation and measurement of the effective chirality parameter of a composite chiral material over a wide frequency band," *IEEE. Trans. Antennas Propagat.*, vol. 43, pp. 123–130, Feb. 1995.

[22] G. J. Burke, "Numerical electromagnetic code NEC-4—Method of moments," Document UCRL-MA-109338, Lawrence Livermore National Laboratory, 1992.

[23] I. P. Theron and J. H. Cloete, "The electric quadrupole contribution to the circular birefringence of nonmagnetic anisotropic chiral media: A circular waveguide experiment," *IEEE Trans. Antennas Propagat.*, vol. 44, pp. 1451–1459, Aug. 1996.

[24] K. W. Whites, "Full-wave computation of constitutive parameters for lossless composite chiral materials," *IEEE Trans. Antennas Propagat.*, vol. 43, pp. 376–384, Apr. 1995.

[25] S. Cornbleet, *Microwave Optics: The Optics of Microwave Antenna Design.* London: Academic, 1976.

[26] F. Guérin, "Microwave chiral materials: A review of experimental studies and some results on composites with ferroelectric ceramic inclusions," in *PIERS Book Series Vol. 9, Bianisotropic and Bi-Isotropic Media and Applications*, A. Priou, Ed., 1994, pp. 219–263.

[27] K. F. Lindman, *Ann. Phys.*, vol. 63, p. 621, 1920.

[28] ———, *Ann. Phys.*, vol. 69, p. 270, 1922.

[29] I. Tinoco and M. P. Freeman, "The optical activity of oriented copper helixes—Part I: Experimental," *J. Chem. Phys.*, vol. 61, pp. 1196–1200, 1957.

[30] A. G. Smith, J. H. Cloete, and I. P. Theron, "The accuracy of a free-space system for measuring the electromagnetic properties of microwave chiral materials," in *Proc. Chiral'95 Conf.*, Pennsylvania State University, Oct. 11–14, 1995, pp. 13–16.

[31] V. V. Varadan, A. Lakhtakia, and V. K. Varadan, "Equivalent dipole moments of helical arrangements of small, isotropic, point-polarizable scatterers: Application to chiral polymer design," *J. Appl. Phys.*, vol. 63, no. 2, pp. 280–284, 1988.

Colin R. Brewitt-Taylor received the B.A. degree in physics and the Ph.D. degree in geophysics from the University of Cambridge, U.K., in 1970 and 1974, respectively.

In 1979, he joined the Royal Signals and Radar Establishment, Malvern, U.K., now subsumed into the U.K. Defense Evaluation and Research Agency, where he still works. He has specialized in electromagnetic theory and associated numerical techniques, with particular interests in planar antennas, electromagnetic scattering, and radar absorbing materials.

Peter G. Lederer received the B.Sc. and Ph.D. degrees in electronic engineering from the University of Wales in 1974 and 1982, respectively.

In 1982, he joined the Royal Signals and Radar Establishment, now subsumed into the U.K. Defense Evaluation and Research Agency, where he still works. Here he studies the modeling and characterization of radar absorbent materials with a particular emphasis on the microwave constitutive parameters of dielectric, magneto-dielectric, and chiral materials and their measurement. Since 1977, his interests have been in the electrical properties of materials. His Ph.D. research at Bangor focused on charge transport mechanisms in biological materials, after which he studied the trapping effects of impurities in semiconductors at the University of Manchester.

Frank C. Smith received the B.Sc. degree in 1983, the M.Sc. degree in 1985, and the Ph.D. degree in 1989.

From 1985 to 1992, he was at the University of Sheffield, U.K., where he worked on microwave absorber measurement techniques, numerical techniques in electromagnetic scattering, and the analysis of large ground-based radomes. From 1993 to 1995 he was at the Defense Evaluation and Research Agency in Malvern, U.K., where he continued his work in novel microwave measurement techniques. Since 1995 he has been a Lecturer at the University of Hull, U.K., specializing in the design and characterization of radar absorbing materials.

Sajad Haq received the B.Sc. (Hons) degree in electronics and electrical engineering from the University of Glasgow, U.K., and the Ph.D. degree in electronic materials from the University of Birmingham, U.K.

Since 1990, he has worked at the Sowerby Research Center, British Aerospace, at Bristol, U.K., on novel electromagnetic materials and devices.